PAPER

Check for updates

Relaxor-like and switchable dielectric behavior in a rare noncentrosymmetric 3D iodoargentate hybrid†

Shan-Shan Yu,‡[a] Shao-Xian Liu,‡[a] Yi-Xiao Zhu,[c] Hai-Bao Duan [iD] *[ab] and H. Zhang*[a]

A rare noncentrosymmetric three-dimensional (3D) iodoargentate hybrid, namely, $[Cd(en)_3]Ag_2I_4$ (**1**), was prepared using a simple solution process. **1** crystallized in the hexagonal space group $P6_322$. Its inorganic components formed a novel 3D open-framework structure. **1** is the first 3D iodoargentate hybrid shown to have relaxor-like dielectric behavior and switchable dielectric properties.

Hybrid iodoargentates have been intensively investigated not only because of their flexible coordination modes and bonding arrangements,[1,2] but also because of their novel physical properties applicable in fields from optics[3] to electronics.[4] Many anionic iodoargentates with the general formula $(Ag_mI_n)^{(n-m)-}$ have been synthesized and structurally characterized, such as zero-dimensional (0D) clusters of $[Ag_4I_8]^{4-}$, $[Ag_5I_9]^{4-}$, $[Ag_5I_{10}]^{5-}$, $[Ag_6I_{12}]^{6-}$ and $[Ag_7I_{13}]^{6-}$,[5,6] one-dimensional (1D) chains of $[AgI_2]^-$, $[Ag_2I_5]^{3-}$, $[Ag_4I_6]^{2-}$, $[Ag_5I_7]^{2-}$ and $[Ag_6I_8]^{2-}$,[7,8] two-dimensional (2D) s of $[Ag_2I_3]^-$, $[Ag_4I_5]^-$, $[Ag_5I_6]^-$ and $[Ag_{11}I_{15}]^{4-}$,[9] and three-dimensional (3D) frameworks of $[AgI_2]^-$, $[Ag_4I_6]^-$ and $[Ag_5I_7]^{2-}$.[3a] Three-dimensional iodoargentates are non-oxide analogues of microporous zeolites and have led to new developments in host–guest chemistry through crystal engineering of the building blocks of their chemical frameworks, but there are few reported examples of 3D iodoargentates. Noncentrosymmetric 3D iodoargentates are of great importance not only due to their interesting structural features but also because they have been exploited in second-order nonlinear, ferroelectric, and other related applications. However, it is still challenging to synthesize noncentrosymmetric 3D iodoargentates, especially to effectively utilize agents that direct the formation of achiral structures.[10]

On the other hand, supramolecular chemistry and molecular crystal engineering, which involve the planning and utilization of crystal-oriented syntheses for the bottom-up construction of functional molecular solids from molecules and ions, are powerful tools that have been used for the assembly of designed functional materials over the past three decades.[11] In our previous study, we focused our research on the haloplumbate hybrids, and some soft organic components were introduced into haloplumbate crystal lattices. Those haloplumbate hybrid compounds showed arresting ferroelectric, dielectric and thermochromic luminescence properties.[12–14] Recent investigation showed localized charged states to be strongly coupled to local structural lattice distortions and cation rotations in haloplumbate hybrid crystals,[15] and to induce dielectric relaxation behavior. Compared to the Pb^{2+} hybrid, Ag^1 with a d^{10} closed-shell electronic configuration has shown flexible arrangements around the metal center and resulting local polar fluctuations have been shown to result in interesting photoelectric properties. Here, we obtained a rare 3D iodoargentate hybrid, namely, $[Cd(en)_3]Ag_2I_4$ (**1**), and characterized its dielectric properties. A frequency-dependent dielectric dispersion phenomenon was observed above room temperature and analyzed using impedance spectroscopy. The dielectric relaxation behavior of **1** may have been due to local polarization effects of the framework. **1** is the first 3D iodoargentate hybrid shown to have dielectric relaxation and switchable dielectric behaviors.

The compound **1** crystal was synthesized by combining a DMF solution of $Cd(NO_3)_2$ and 2 ml of an ethylenediamine and $KAgI_2$/DMF solution. The resulting solution was kept at room temperature for two weeks, and white block crystals were formed in *ca.* 90% yield based on CD (see ESI†). The phase purity of the as-prepared sample was characterized by carrying out powder X-ray diffraction (PXRD), elemental analyses of C, H and N, and IR spectroscopy (Fig. S1†). TG was used to analyze its stability up to 300 °C (Fig. S2†). The second-order nonlinear optical properties for **1** were examined, and indicated that the

[a]Key Laboratory of Advanced Functional Materials of Nanjing, Nanjing Xiaozhuang University, Nanjing 211171, P. R. China. E-mail: duanhaibao4660@163.com

[b]Department of Chemistry and Biochemistry, University of California, Los Angeles, California 90095-1569, USA

[c]Nanjing Foreign Language School, Nanjing 210018, P. R. China

‡ Shan-Shan Yu and Shao-Xian Liu contribute equally.

powdered samples of **1** were SHG active with a response *ca.* 0.5 times that of urea.§

Compound **1** crystallized in the hexagonal space group $P6_322$ (no. 182), which belongs to the chiral point group D_6, and with an asymmetric unit containing two crystallographically distinct Ag^+ ions and two crystallographically distinct I^- ions together with one dication complex (as depicted in Fig. 1a). The inorganic part of **1** formed a novel 3D open-framework structure, made up of tetrahedral AgI_4 building blocks. The Ag–I bond length was measured to be in the range 2.882–2.892 Å, all within the van der Waals contact limit. The Ag–I–Ag bond angles ranged from 104.7 to 113.7°, slightly deviating from 109.5° for an ideal tetrahedron. All of the I^- anions formed μ_2 bridges connecting two neighboring Ag^+ ions. Thus, each Ag_1I_4 tetrahedron shared its vertex with another four different Ag_2I_4 tetrahedra (Fig. 1b). Six AgI_4 tetrahedra were observed to stack into a 12-ring structure (Fig. 1c), and a non-interpenetrating tridymite-type topology formed from the 12-ring structure. Along the *a*- and *b*-axis directions, an approximately rectangular inorganic channel was observed and measured to have dimensions of about 5.77 × 9.25 Å without considering internal van der Waals radii (Fig. 1d and e). Furthermore, another irregular 12-ring channel formed along the *c* axis (Fig. 1f). The channels along the three directions were observed to merge into a 3D channel network, a rare example of an open silver halide framework, and $Cd(en)_3^{2+}$ dications filled the channels (Fig. 1e). The Cd^{2+} ions of the $Cd(en)_3^{2+}$ dications were observed to occupy the Wyckoff position, its coordination octahedron, with a C_3 point group symmetry, was built from six nitrogen atoms from three ethylenediamine molecule. Charged H-bonding interactions formed between the dications and 3D inorganic framework.

Dielectric relaxation investigation were carried out for temperatures between 50 and 140 °C using the complex modulus (Fig. 2 and S4†). The electric modulus (M^*) was calculated according to the equation

$$M^*(\omega) = \frac{1}{\varepsilon^*(\omega)} = \frac{\varepsilon' + j\varepsilon''}{\varepsilon'^2 + \varepsilon''^2} = M' + jM'',$$

where M' and M'' are the real and imaginary parts of the complex modulus M^*, respectively. At low frequencies, M' was calculated to be very small, to indicative of negligible contributions of the electrode polarization and space charge injection effects. The M' showed a tendency to saturate at high frequencies, which is typical for dielectric relaxation process in the investigated temperature range (Fig. 2a). The shift of the M' maximum slightly toward a higher temperature upon
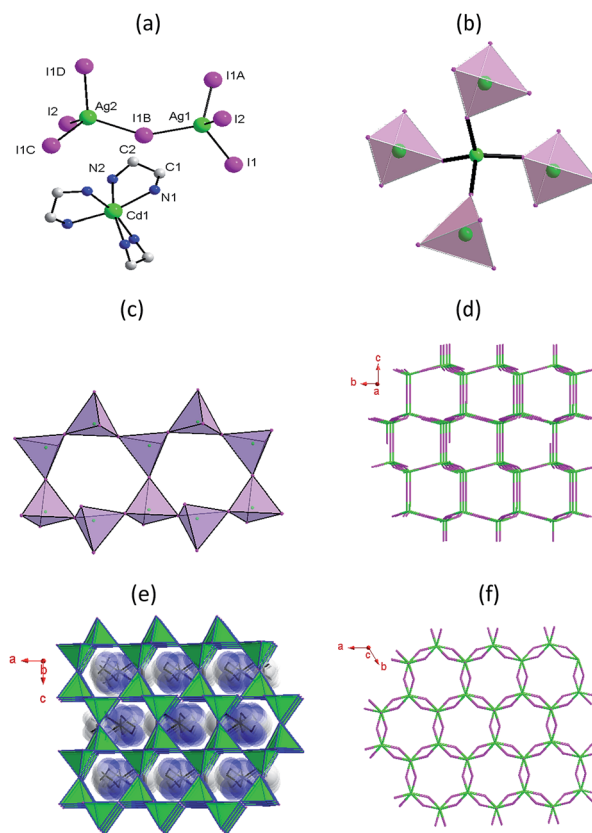
Fig. 1 (a) The asymmetric unit of **1** at 293 K with 50% thermal ellipsoid probability. (b) Each AgI_4 tetrahedron was observed to share its vertex with another four different AgI_4 tetrahedra. (c) 12-ring structure formed by six AgI_4 tetrahedra. (d) View of an approximately rectangular inorganic channel along the *a*-axis direction. Dications in the channel are omitted for clarity. (e) Packing structure along the *b*-axis, with $Cd(en)_3^{2+}$ dications filling the channels and shown in space-filling mode. (f) Another irregular channel along the *c*-axis. (Symmetry relationships: $A = -x, 1-y, -z; B = 1-x, 1-y, 1+z; C = 1-x, 1+y, z; D = x, -y, 0.5-z$.)

increasing the frequency of the applied electrical field further indicated a thermally activated process. Furthermore, the contribution of conduction to frequency was due to the short-range mobility of the charge carriers. In the M''–f plots, the spectrum at the investigated temperature exhibited a relaxation peak (Fig. 2b). The peaks shifted systematically towards higher frequencies as the temperature was increased. This shift implied a redevelopment of the polarization at high temperature, and thus the occurrence of relaxation at high frequency. In order to gain deep insight into the dielectric relaxation process, the frequency dependence of the peak for M'' at different temperatures was plotted (Fig. 2c) according to the relationship

$$\tau = \tau_0 \exp\left(\frac{E_a}{k_B T}\right). \tag{1}$$

In this equation, $\tau = 1/f_{max}$, where f_{max} is the frequency at the maximum of M''–f in the plot at temperature T, τ_0 represents the characteristic macroscopic relaxation time, E_a is the activation energy or potential barrier required for the dielectric relaxation,
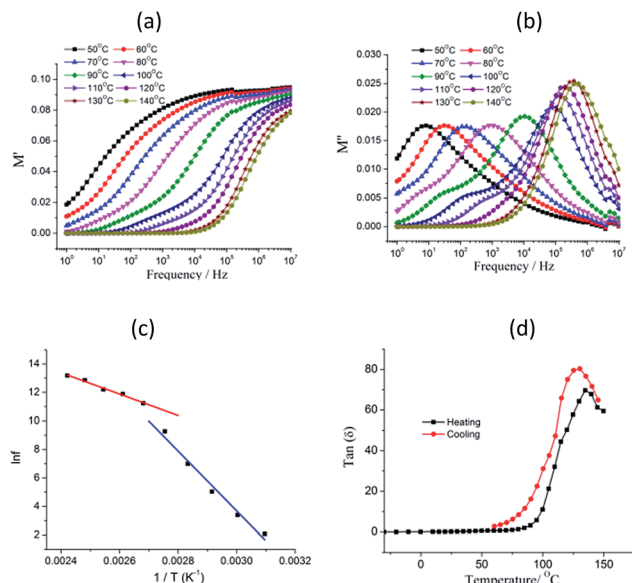
Fig. 2 (a and b) Frequency dependencies of the M' and M'' of 1 in the 50–140 °C temperature range, respectively. (c) Plots of ln f vs. $1/T$ for the relaxation at selected temperatures and (d) tan(δ) versus temperature at 100 Hz for 1.

and k_B is Boltzmann's constant. Two steps of dielectric relaxation were found, as shown in Fig. 2c. We found $\ln f_{max}$ to be linearly related to $1/T$ in the temperature ranges 323–363 K and 373–413 K. The best fits gave the following results: $\tau_0 = 1.356 \times 10^{-29}$ s and $E_a = 21.07$ kcal mol^{-1} in the temperature range 323–363 K and $\tau_0 = 2.15 \times 10^{-14}$ s and $E_a = 7.53$ kcal mol^{-1} in the temperature range 373–413 K. The dielectric relaxation process was also indicated from the tan(δ)–f plot (tan(δ) = $\varepsilon''/\varepsilon'$) (Fig. S3†), which showed a broad maximum at the selected temperature, and the maximum tan(δ) peak shifted toward higher frequencies as the temperature was increased, indicating the occurrence of thermally active dielectric relaxation. However, the frequency dependence of tan(δ) showed a strong low-frequency dispersion when the temperature was increased (Fig. S3†). When the temperature is above 100 °C, the dielectric loss shows abrupt increase, which reaches the values of 6.31 for 1 and 10 Hz. The temperature-dependent dielectric loss is shown in Fig. 2d. When the frequency was lower than 100 Hz, an obvious dielectric anomaly was present at about 135 °C in the heating process. As the temperature was further increased, the tan(δ) value decreased. During the subsequent cooling process, a small thermal hysteresis was obtained. The dielectric loss switching between high and low dielectric states and the thermal hysteresis indicated compound 1 to be a potential switchable bistable dielectric material.

In general, four different mechanisms for dielectric relaxation have been proposed. The electronic polarization and molecular vibration occurred at frequencies above 10^{12} Hz. At the frequency range of 10^6–10^{12} Hz, the dielectric relaxation was more prevalent than dipole motion or ionic polarization. Dielectric relaxation is usually found in disordered solids such as relaxor ferroelectrics, dipolar glass and inorganic–organic

hybrids, and can be ascribed to order–disorder phase transition; some metal–organic frameworks and ionic cocrystals also show dielectric relaxation behavior.[16] However, we were surprised to observe relaxor-like behavior in compound 1, which was shown to not have a disordered component; and the DSC results (Fig. S5†) indicated the absence of a phase transition in the investigated temperature range. In compound 1, Ag and I ions were observed to have large ion displacements, the 3D channel structure formed by compound 1 became more distorted as the temperature was increased. Thus, we suggested the dielectric relaxation behavior of 1 to be associated with local polarization effects due to the flexibility of the channel structure and, in particular, due to small local movements of the Ag and I ions in the framework to create local dipole moments.

The abrupt increase in dielectric loss at 100 Hz above 100 °C. The dielectric loss reached a value of 10.25 at 105 °C, was due to the electronic conductance.[17] To further investigate the dielectric and conduction behaviors of compounds 1, the complex impedance (Z'–Z'') at selected temperatures was plotted (Fig. 3a and b). The semicircles were observed for the selected temperature. The low-frequency dispersion corresponded to the grain boundary and the high-frequency region corresponded to the grain interior. This observation indicated that a single conductivity process took place in the sample at the investigated frequency. The impedance spectra from Fig. 3a and b were interpreted by means of an equivalent circuit. Here, each impedance semicircle represents the total dc resistance of the sample, R, furthermore, bulk capacitor, C in parallel (parallel RC element) and C_x (Cole–Cole branch) represents polarization associated with the lattice relaxation process. The centers of these semicircles were located below the real axis, indicating a non-Debye type of relaxation process. The best fit to the data
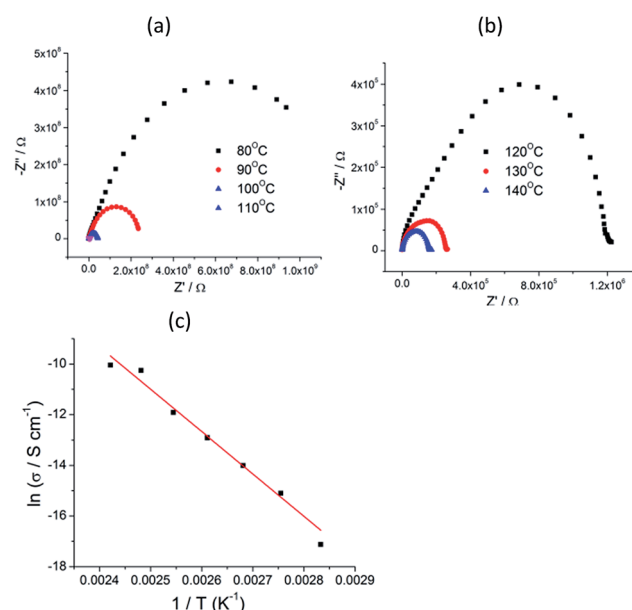

Fig. 3 (a and b) Complex-plane impedance plots at various temperatures. (c) Temperature dependence of conductivity for 1 (black dot: obtained from using an equivalent circuit; red line: theoretically reproduced using the Arrhenius equation).

gave $\sigma = 3.63 \times 10^{-8}$ S cm^{-1} at 353 K for **1**. As the temperature was increased, the electrical conductivity continuously increased, by a total of about three orders of magnitude to 4.35×10^{-5} S cm^{-1} for **1** at 413 K. We found ln σ of **1** to be linearly related to $1/T$ between 353 K and 413 K (Fig. 3c), and its activation energy (E_a) was estimated to be 25.8 kcal mol^{-1}.

In summary, compound [Cd(en)$_3$]Ag$_2$I$_4$ (**1**) was successfully prepared by using a simple self-assembly method. Compound **1** represents a rare noncentrosymmetric 3D framework hybrid iodoargentate with a metal complex as a template. Furthermore, **1** showed relaxor-like dielectric behavior and switchable dielectric properties in the investigated temperature range, and dielectric relaxation behavior was associated with local polarization effects due to the flexibility of the channel structure and small local movement of the Ag and I ions in the framework to create local dipole moments. These results revealed hybrid iodoargentates to have interesting relaxor-like properties and to be of potential use as switchable dielectric materials.

Conflicts of interest

There are no conflicts to declare.

Acknowledgements

Notes and references

1 (a) S. Mishra, E. Jeanneau, G. Ledoux and S. Daniele, *Inorg. Chem.*, 2014, **53**, 11721–11731; (b) H. H. Li, Y. Y. Xing, Z. X. Lian, A. W. Gong, H. Y. Wu, Y. Li and Z. R. Chen, *CrystEngComm*, 2013, **15**, 1721–1728; (c) T. Yu, Y. B. Fu, Y. L. Wang, P. F. Hao, J. J. Shen and Y. L. Fu, *CrystEngComm*, 2013, **17**, 8752–8761.

2 (a) J. J. Shen, C. F. Zhang, T. L. Yu, L. An and Y. L. Fu, *Cryst. Growth Des.*, 2014, **14**, 6337–6342; (b) T. L. Yu, J. J. Shen, Y. L. Wang and Y. L. Fu, *Eur. J. Inorg. Chem.*, 2015, **2015**, 1989–1996.

3 (a) Z. Wang, G. L. Zhuang, Y. K. Deng, Z. Y. Feng, Z. Z. Cao, M. Kurmoo, C. H. Tung and D. Sun, *Inorg. Chem.*, 2016, **55**, 4757–4763; (b) Z. H. Yan, X. Y. Li, L. W. Liu, S. Q. Yu, X. P. Wang and D. Sun, *Inorg. Chem.*, 2016, **55**, 1096–1101; (c) X. W. Lei, C. Y. Yue, J. Zhang, Y. F. Han, J. T. Yang, R. R. Meng, C. S. Gao, H. Ding, C. Y. Wang, W. D. Chen and M. C. Hong, *Inorg. Chem.*, 2015, **54**, 10593–10603.

4 T. Devic, M. Evain, Y. Moelo, E. Canadell, P. Auban-Senzier, M. Fourmigué and P. Batail, *J. Am. Chem. Soc.*, 2003, **125**, 3295–3301.

5 (a) S. Mishra, E. Jeanneau, G. Ledoux and S. Daniele, *Inorg. Chem.*, 2014, **53**, 11721–11731; (b) H. H. Li, Y. Y. Xing, Z. X. Lian, A. W. Gong, H. Y. Wu, Y. Li and Z. R. Chen, *CrystEngComm*, 2013, **15**, 1721–1728.

6 (a) W. X. Xu, W. X. Zhou, J. Li, S. L. Huang, J. Niu and F. X. Zhang, *Inorg. Chem. Commun.*, 2014, **40**, 220–222; (b) T. L. Yu, J. J. Shen, Y. B. Fu and Y. L. Fu, *CrystEngComm*, 2014, **16**, 5280–5289.

7 (a) G. N. Liu, L. L. Liu, Y. N. Chu, Y. Q. Sun, Z. W. Zhang and C. C. Li, *Eur. J. Inorg. Chem.*, 2015, **2015**, 478–487; (b) L. Li, H. Chen, Y. Z. Qiao and Y. Y. Niu, *Inorg. Chim. Acta*, 2014, **409**, 227–232; (c) W. Fang, C. Y. Tang, R. H. Chen, D. X. Jia, W. Q. Jiang and Y. Zhang, *Dalton Trans.*, 2013, **42**, 15150–15158.

8 R. C. Zhang, Y. J. Zhang, B. Q. Yuan, J. P. Miao, B. H. Pei, P. P. Liu, J. J. Wang and D. J. Zhang, *J. Solid State Chem.*, 2014, **220**, 185–190.

9 (a) T. L. Yu, L. An, L. Zhang, J. J. Shen, Y. B. Fu and Y. L. Fu, *Cryst. Growth Des.*, 2014, **14**, 3875–3879; (b) X. W. Lei, C. Y. Yue, L. J. Feng, Y. F. Han, R. R. Meng, J. T. Yang, H. Ding, C. S. Gao and C. Y. Wang, *CrystEngComm*, 2016, **18**, 427–436; (c) E. Cariati, R. Macchi, D. Roberto, R. Ugo, N. Casati, P. Macchi, A. Sironi, L. Bogani, A. Caneschi and D. Gatteschi, *J. Am. Chem. Soc.*, 2007, **129**, 9410–9420.

10 Y. S. Jiang, H. G. Yao, S. H. Ji, M. Ji and Y. L. An, *Inorg. Chem.*, 2008, **47**, 3922–3924.

11 (a) A. M. Guloy, Z. J. Tang, P. B. Miranda and V. I. Srdanov, *Adv. Mater.*, 2001, **13**, 833–837; (b) T. P. Radhakrishnan, *Acc. Chem. Res.*, 2008, **41**, 367–376; (c) G. R. Desiraju, *Angew. Chem., Int. Ed.*, 2007, **46**, 8342–8356.

12 H. B. Duan, H. R. Zhao, X. M. Ren, H. Zhou, Z. F. Tian and W. Q. Jin, *Dalton Trans.*, 2011, **40**, 1672–1683.

13 Y. B. Tong, L. T. Ren, H. B. Duan, J. L. Liu and X. M. Ren, *Dalton Trans.*, 2015, **44**, 17850–17858.

14 H. B. Duan, S. S. Yu, Y. B. Tong, H. Zhou and X. M. Ren, *Dalton Trans.*, 2016, **45**, 4810–4818.

15 (a) A. J. Neukirch, W. Nie, J. C. Blancon, K. Appavoo, H. Tsai, M. Y. Sfeir, C. Katan, L. Pedesseau, J. Even, J. J. Crochet, G. Gupta, A. D. Mohite and S. Tretiak, *Nano Lett.*, 2016, **16**, 3809–3816; (b) O. Yaffe, Y. S. Guo, L. Z. Tan, D. A. Egger, T. Hull, C. C. Stoumpos, F. Zheng, T. F. Heinz, L. Kronik, M. G. Kanatzidis, J. S. Owen, A. M. Rappe, M. A. Pimenta and L. E. Brus, *Phys. Rev. Lett.*, 2017, **118**, 136001-1–136001-6.

16 (a) D. W. Fu, W. Zhang, H. L. Cai, Y. Zhang, J. Z. Ge, R. G. Xiong, S. P. Huang and T. Nakamura, *Angew. Chem., Int. Ed.*, 2011, **50**, 11947–11951; (b) Z. H. Sun, T. L. Chen, J. H. Luo and M. C. Hong, *Angew. Chem., Int. Ed.*, 2012, **51**, 3871–3876.

17 (a) J. C. Papaioannou and T. C. Ghikas, *Mol. Phys.*, 2003, **101**, 260–2608; (b) T. C. Ghikas and J. C. Papaioannou, *Mol. Phys.*, 2002, **100**, 673–679; (c) C. Ang and Z. Yu, *Phys. Rev. B: Condens. Matter Mater. Phys.*, 2000, **61**, 3922.